

[³H]Epibatidine Photolabels Non-equivalent Amino Acids in the Agonist Binding Site of *Torpedo* and $\alpha 4\beta 2$ Nicotinic Acetylcholine Receptors*[§]

Received for publication, May 12, 2009, and in revised form, June 24, 2009. Published, JBC Papers in Press, July 20, 2009, DOI 10.1074/jbc.M109.019083

Shouryadeep Srivastava^{‡1}, Ayman K. Hamouda^{§1}, Akash Pandhare[‡], Phaneendra K. Duddempudi[‡], Mitesh Sanghvi[‡], Jonathan B. Cohen[§], and Michael P. Blanton^{‡2}

From the [‡]Department of Pharmacology and Neuroscience and the Center for Membrane Protein Research, School of Medicine, Texas Tech University Health Sciences Center, Lubbock, Texas 79430 and the [§]Department of Neurobiology, Harvard Medical School, Boston, Massachusetts 02115

Nicotinic acetylcholine receptor (nAChR) agonists, such as epibatidine and its molecular derivatives, are potential therapeutic agents for a variety of neurological disorders. In order to identify determinants for subtype-selective agonist binding, it is important to determine whether an agonist binds in a common orientation in different nAChR subtypes. To compare the mode of binding of epibatidine in a muscle and a neuronal nAChR, we photolabeled *Torpedo* $\alpha 2\beta\gamma\delta$ and expressed human $\alpha 4\beta 2$ nAChRs with [³H]epibatidine and identified by Edman degradation the photolabeled amino acids. Irradiation at 254 nm resulted in photolabeling of α Tyr¹⁹⁸ in agonist binding site Segment C of the principal (+) face in both α subunits and of γ Leu¹⁰⁹ and γ Tyr¹¹⁷ in Segment E of the complementary (–) face, with no labeling detected in the δ subunit. For affinity-purified $\alpha 4\beta 2$ nAChRs, [³H]epibatidine photolabeled $\alpha 4$ Tyr¹⁹⁵ (equivalent to *Torpedo* α Tyr¹⁹⁰) in Segment C as well as $\beta 2$ Val¹¹¹ and $\beta 2$ Ser¹¹³ in Segment E (equivalent to *Torpedo* γ Leu¹⁰⁹ and γ Tyr¹¹¹, respectively). Consideration of the location of the photolabeled amino acids in homology models of the nAChRs based upon the acetylcholine-binding protein structure and the results of ligand docking simulations suggests that epibatidine binds in a single preferred orientation within the α - γ transmitter binding site, whereas it binds in two distinct orientations in the $\alpha 4\beta 2$ nAChR.

Nicotinic acetylcholine receptors (nAChRs)³ are prototypical members of the Cys loop superfamily of neurotransmitter-

gated ion channels that mediate the actions of the neurotransmitter acetylcholine (1). nAChRs from vertebrate skeletal muscle and the electric organs of *Torpedo* rays are heteropentamers of homologous subunits with a stoichiometry of $2\alpha:\beta:\gamma(\epsilon):\delta$ that are arranged pseudosymmetrically around central cation-selective ion channels (1, 2). There are 12 mammalian neuronal nAChR subunit genes: nine neuronal α subunits ($\alpha 2$ – $\alpha 10$) and three neuronal β subunits ($\beta 2$ – $\beta 4$). The $\alpha 4\beta 2$ nAChR is the most abundant and widely distributed nAChR subtype expressed in the brain and is a major target for potential therapeutic agents for neurological diseases and conditions, including nicotine dependence and Alzheimer and Parkinson diseases (3, 4). Although the ratio of $\alpha 4$ to $\beta 2$ subunit *in vivo* is uncertain, expressed receptors containing either three $\alpha 4$ or three $\beta 2$ subunits have distinct pharmacological properties (5, 6).

The agonist binding sites (ABS) of nAChRs are located within the amino-terminal extracellular domain at the interface of adjacent subunits (α - γ and α - δ in the *Torpedo* nAChR), and different nAChR subunit combinations form ABS with distinct physical and pharmacological properties (3, 7). Affinity labeling studies with *Torpedo* nAChR and site-directed mutational analyses of muscle and neuronal nAChRs identified key amino acids delineating the ABS from three noncontiguous stretches of the α subunit (Segments A–C, the principal component (+ face)) and three noncontiguous regions of the non- α subunit (Segments D–F, the complementary component (– face)) (8, 9). The three-dimensional structure of the ABS in the absence and presence of nAChR agonists or competitive antagonists has been determined for snail acetylcholine-binding proteins (AChBPs) that are soluble homopentamers homologous to the extracellular (amino-terminal) domain of a nAChR (10–12). In the AChBP, four aromatic amino acids from Segments A–C that are conserved within α subunits, along with a conserved Trp in Segment D, form a core aromatic “pocket” with a dimension optimal for accommodation of a trimethylammonium group. The other amino acids in the non- α subunits closest to the aromatic pocket, which are generally not conserved among γ , δ , or neuronal β subunits, are on three antiparallel β strands. The AChBP structure was used to refine the structure of the *Torpedo* nAChR in the absence of agonist to 4 Å resolution (13). In this structure, there is a reorientation of Segments A–C, resulting in the absence of a well defined core aromatic binding pocket.

* This work was supported, in whole or in part, by National Institutes of Health Grant GM-58448 (to J. B. C.). This work was also supported in part by American Heart Association South Central Affiliate Grant-in-Aid 0755029Y (to M. P. B.) and the South Plains Foundation (to M. P. B.).

§ The on-line version of this article (available at <http://www.jbc.org>) contains supplemental Figs. S1–S3.

¹ Both authors contributed equally to this work.

² To whom correspondence should be addressed: Dept. of Pharmacology and Neuroscience, Texas Tech University Health Sciences Center, 3601 4th St., Lubbock, TX 79430. Tel.: 806-743-2425; Fax: 806-743-2744; E-mail: michael.blanton@ttuhsc.edu.

³ The abbreviations used are: nAChR, nicotinic acetylcholine receptor; HEK- $\alpha 4\beta 2$, human $\alpha 4\beta 2$ nAChR(s); ABS, agonist binding sites; ACh, acetylcholine; AChBP, acetylcholine-binding protein; dTC, D-tubocurarine; V8 protease, *S. aureus* endopeptidase Glu-C; EndoLys-C, endoproteinase Lys-C; OPA, *o*-phthalaldehyde; VDB, vesicle dialysis buffer; HPLC, high performance liquid chromatography; rpHPLC, reverse phase high performance liquid chromatography; CHAPS, 3-[(3-cholamidopropyl)dimethylammonio]-1-propanesulfonic acid; MOPS, 4-morpholinepropanesulfonic acid.

Binding Modes of [³H]Epibatidine to Muscle and Neuronal nAChRs

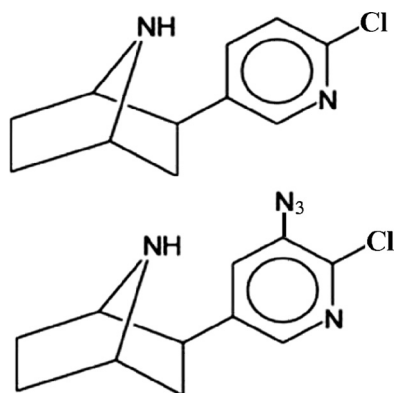


FIGURE 1. Structure of [³H]epibatidine (top) and azidoepibatidine (bottom).

Analysis of agonist interactions with mutant nAChRs containing fluorine-substituted core aromatic residues provides evidence that cation- π interactions, particularly with α Trp¹⁴⁹ in Segment B, are important determinants of agonist binding affinity (14) and for the higher affinity binding of nicotine to $\alpha 4\beta 2$ nAChRs compared with $\alpha 2\beta\gamma\delta$ nAChRs (15). Mutational analyses and molecular docking calculations have also provided evidence that two molecules of very similar structure may actually bind to a single receptor in very different orientations, as seen for two high affinity antagonists, D-tubocurarine and its quaternary ammonium analog metocurine, binding to the AChBP and to the muscle nAChR (16, 17).

Photoaffinity labeling provides an alternative means to identify amino acids contributing to a drug binding site (18, 19) and has been used to determine the orientation of drugs bound in the ABS of *Torpedo* nAChR (20). Epibatidine binds with very high affinity (~ 10 pM) to heteromeric neuronal nAChRs (e.g. $\alpha 4\beta 2$) and with nanomolar affinity to $\alpha 7$ and muscle-type/*Torpedo* nAChRs (3). Utilizing a photoreactive analogue of epibatidine (azidoepibatidine; Fig. 1) and mass spectrometry, Tomizawa *et al.* (21) identified photolabeled amino acids in the *Aplysia* AChBP (Tyr¹⁹⁵ in Segment C and Met¹¹⁶ in Segment E), establishing an orientation for bound azidoepibatidine consistent with the orientation of epibatidine in an AChBP crystal structure (12).

In this report, we use [³H]epibatidine as a photoaffinity reagent to identify the amino acids photolabeled in an expressed $\alpha 4\beta 2$ nAChR and in the *Torpedo* $\alpha 2\beta\gamma\delta$ nAChR. Comparisons of the labeled amino acids seen in the *Torpedo* nAChR α - γ binding site and in the $\alpha 4\beta 2$ nAChR, in conjunction with the results of docking calculations for epibatidine binding to homology models of the $\alpha 2\beta\gamma\delta$ and $\alpha 4\beta 2$ nAChRs, suggests that epibatidine binds in a single orientation in the α - γ site but in two orientations in the $\alpha 4\beta 2$ ABS.

EXPERIMENTAL PROCEDURES

Materials—[³H]Epibatidine (45 Ci/mmol) was obtained from PerkinElmer Life Sciences and stored in 95% ethanol at 4 °C. Carbamylcholine chloride, bromoacetylcholine bromide, and diisopropylfluorophosphate were from Sigma. Epibatidine and D-tubocurarine (dTC) were from Tocris (Ellisville, MO), and *Staphylococcus aureus* endoproteinase Glu-C (V8 protease) was from Worthington. Endoproteinase Lys-C (EndoLys-C) and protease

inhibitor mixture set III were from Calbiochem. Sodium cholate and CHAPS were from U.S. Biochemical Corp. Affi-Gel 10 was from Bio-Rad. Synthetic lipids (dioleoyl phosphatidic acid and dioleoyl phosphatidylcholine) as well as cholesterol, asolectin, and total lipid extract from porcine brain were obtained from Avanti Polar Lipids (Alabaster, AL).

Preparation of *Torpedo* nAChR—*Torpedo californica* nAChR-rich membranes for radioligand binding studies and for affinity purification were isolated from frozen electric organs (Aquatic Research Consultants, San Pedro, CA), as described previously (22). *Torpedo* nAChR-rich membranes at 1 mg/ml protein were solubilized in 1% sodium cholate in vesicle dialysis buffer (VDB; 100 mM NaCl, 0.1 mM EDTA, 0.02% NaN₃, 10 mM MOPS, pH 7.5) and treated with 0.1 mM diisopropylfluorophosphate after insoluble material was pelleted by centrifugation (91,000 $\times g$ for 1 h). The nAChR was affinity-purified on a bromoacetylcholine bromide-derivatized Affi-Gel 10 column and then reconstituted into lipid vesicles composed of dioleoyl phosphatidic acid/dioleoyl phosphatidylcholine/cholesterol (at a molar ratio of 3:1:1), as described (23, 24). The lipid/nAChR ratio was adjusted to molar ratio of 400:1. Based upon SDS-PAGE, after purification, the nAChR comprised more than 90% of the protein in the preparation. Both the nAChR-rich membranes and purified nAChRs were stored at -80 °C.

Preparation of $\alpha 4\beta 2$ nAChR—HEK-293 cells stably transfected with human $\alpha 4\beta 2$ nAChRs (HEK-h $\alpha 4\beta 2$) were kindly provided by Dr. Joseph H. Steinbach (Department of Anesthesiology, Washington University School of Medicine, St. Louis, MO) (25). HEK-h $\alpha 4\beta 2$ cells were grown at 37 °C in a humidified incubator at 5% CO₂ in 140-mm dishes and maintained in Dulbecco's modified Eagle's medium/Ham's F-12 medium (Mediatech, Herndon, VA) supplemented with 10% fetal bovine serum, 100 units/ml penicillin G, 100 μ g/ml streptomycin, and 450 μ g/ml Geneticin (G418; A.G. Scientific, San Diego, CA) as a selection agent (26). For membrane preparation, HEK-h $\alpha 4\beta 2$ cells were homogenized in VDB in the presence of 0.2 μ l/ml protease inhibitor mixture set III (Calbiochem). Membrane fractions were isolated by centrifugation (39,000 $\times g$ for 1 h) and then resuspended in VDB containing 0.2 μ l/ml protease inhibitor mixture III and stored at -80 °C. For affinity purification, HEK-h $\alpha 4\beta 2$ cell membranes (typically 2 g of protein from ~ 600 dishes) at 1 mg/ml protein in VDB containing 0.2 μ l/ml protease inhibitor mixture III were solubilized with 1% CHAPS, centrifuged (91,500 $\times g$ for 1 h) to pellet insoluble material, and then dialyzed for 5 h against 1% cholate. The h $\alpha 4\beta 2$ nAChRs were affinity-purified on a bromoacetylcholine bromide-derivatized Affi-Gel 10 column and reconstituted into lipid vesicles composed of asolectin/total lipid extract from porcine brain, as described previously (26). The purity of h $\alpha 4\beta 2$ nAChRs was $>50\%$, as estimated by densitometric quantification of Coomassie Blue-stained gels.

Radioligand Binding to *Torpedo* nAChR-rich Membranes—The effect of epibatidine and dTC on the binding of [³H]epibatidine to *Torpedo* nAChR-rich membranes was determined using a centrifugation assay with duplicate samples. Membranes at 0.1 mg/ml protein (16 nM ACh binding sites) in *Torpedo* physiological saline (250 mM NaCl, 5 mM KCl, 3 mM CaCl₂, 2 mM MgCl₂, and 5 mM sodium phosphate, pH 7.0) were incu-

bated for 1 h at room temperature with either 0.5 nM [³H]epibatidine and increasing concentrations of epibatidine (final concentrations 0.3 nM to 3 μM) or 2 nM [³H]epibatidine in the absence and presence of 6 μM proadifen and increasing concentrations of dTC (final concentrations 1 nM to 1 mM). Bound and free [³H]epibatidine were separated by centrifugation (39,000 × *g* for 1 h) and then quantified by liquid scintillation counting. Nonspecific binding was determined in the presence of 1 mM carbamylcholine.

Data Analysis—The concentration-dependent inhibition of [³H]epibatidine binding by epibatidine and dTC were fit according to a single-site model as follows,

$$f_{(x)} = NS + (T/(1 + (x/IC_{50}))) \quad (\text{Eq. 1})$$

and to a two-site model,

$$f_{(x)} = NS + (0.5T/(1 + (x/IC_{50(1)}))) + (0.5T/(1 + (x/IC_{50(2)}))) \quad (\text{Eq. 2})$$

where $f_{(x)}$ is the [³H]epibatidine binding in the presence of competitor concentration x , T is the total specific binding, NS is the nonspecific binding determined in the presence of 1 mM carbamylcholine, and IC_{50} is the concentration of competitor that inhibits 50% of the total specific binding. Sigmaplot version 11 (Systat Software) was used for non-linear least squares fit of the data, and the S.E. values of the parameter fits are indicated.

[³H]Epibatidine Photolabeling of *Torpedo* nAChR—For analytical labelings, ~50-μg samples of affinity-purified *Torpedo* nAChRs in 1 ml of VDB were incubated with 0.13 μM [³H]epibatidine in the absence or presence of epibatidine (40 μM) or increasing concentrations of dTC (final concentrations 0.2–20 μM). After a 2-h incubation at room temperature, the samples in glass test tubes were irradiated for 30 min with a 254-nm UV lamp (Spectroline EN-280L). The labeled membranes were then pelleted by centrifugation (39,000 × *g* for 1 h), resuspended in electrophoresis sample buffer (12.5 mM Tris-HCl, 2% SDS, 8% sucrose, 1% glycerol, 0.01% bromphenol blue, pH 6.8), and resolved on 1-mm-thick, 8% polyacrylamide, 0.33% bisacrylamide gels (27). After staining with Coomassie Blue R-250 and destaining to visualize bands, gels were impregnated with fluor (Amplify; GE Biosciences) for 30 min, dried, and exposed to Eastman Kodak Co. X-Omat LS film at –80 °C (1–4-week exposure). For some 8% gels, following staining and destaining, gels were soaked in distilled water overnight, and bands corresponding to the α and γ subunits were excised, soaked in overlay buffer (5% sucrose, 125 mM Tris-HCl, 0.1% SDS, pH 6.8) for 30 min, transferred to the wells of a 15% acrylamide mapping gel, and digested in gel with 10 μg of V8 protease (28). After electrophoresis, mapping gels were processed for fluorography (3–6-week exposure) as described above. For both 8 and 15% mapping gels, to quantify the amount of ³H cpm incorporated into nAChR subunits or subunit proteolytic fragments, bands were excised from the gel, transferred to 5-ml scintillation vials, and soaked in 0.5 ml of 0.1% SDS for 4 days with occasional mixing. Then 3 ml of liquid scintillation mixture was added, and samples were counted for 5 min.

For labeling on a preparative scale, affinity-purified *Torpedo* nAChRs (~3 mg of protein in 8 ml) were labeled with 550 nM

[³H]epibatidine, and the α and γ subunits were isolated by SDS-PAGE and then subjected to in-gel digestion with V8 protease. Based on fluorographs of mapping gels from analytical scale labeling experiments, labeled proteolytic fragments from each subunit (αV8-20 and γV8-14) were excised, and the polypeptides were retrieved by passive diffusion into 25 ml of elution buffer (0.1 M NH₄HCO₃, 0.1% (w/v) SDS, 1% β-mercaptoethanol, pH 7.8) and concentrated in Centriprep-10 and Centricon-3 concentrators (10/3 kDa cut-off; Amicon) to a final volume of ~150 μl. For digestion with EndoLys-C, αV8-20-labeled peptides were acetone-precipitated (75% acetone at –20 °C overnight) to remove SDS, resuspended in 150 μl of 25 mM Tris-HCl, 0.5 mM EDTA, 0.1% SDS, pH 8.6, and then digested with three units of EndoLys-C for 7 days.

[³H]Epibatidine Photolabeling of α4β2 nAChR—For analytical labelings, ~50-μg samples of affinity-purified α4β2 nAChRs in 1 ml of VDB were photolabeled with 880 nM [³H]epibatidine in the absence or presence of epibatidine (40 μM). For labeling on a preparative scale, α4β2 nAChRs (1.2 mg of protein in 6 ml) were photolabeled with 800 nM [³H]epibatidine. Using the same protocols described above for *Torpedo* nAChR, samples from analytical labelings were processed to determine ³H incorporation into the α4 and β2 nAChR subunits (as well as a 36-kDa proteolytic fragment), and the α4 and β2 nAChR subunits and the 36-kDa proteolytic fragments from preparative scale labeling were retrieved, acetone-precipitated, and resuspended in 150 μl of 0.1 M NH₄HCO₃, 0.1% SDS, pH 7.8, for digestion with V8 protease (100 μg of protease for 4 days).

Reversed-phase HPLC Purification and Sequence Analysis—Prior to sequence analysis, all of the [³H]epibatidine-labeled peptides were purified using reversed-phase HPLC (rpHPLC) on a Shimadzu LC-10A binary HPLC system, using a Brownlee Aquapore C₄ column (100 × 2.1 mm). Solvent A was composed of 0.08% trifluoroacetic acid in water, and Solvent B contained 0.05% trifluoroacetic acid in 60% acetonitrile, 40% 2-propanol. A non-linear elution gradient at 0.2 ml/min was employed (25–100% Solvent B in 100 min, shown as *dotted line* in the figures), and fractions were collected every 2.5 min (40 fractions/run). The elution of peptides was monitored by the absorbance at 210 nm, and the amount of ³H associated with each fraction was determined by liquid scintillation counting of 5% aliquots.

For sequence analysis, rpHPLC fractions containing peaks of ³H were pooled, diluted 3-fold with 0.1% trifluoroacetic acid, and loaded onto polyvinylidene difluoride filters using Prosorb® sample preparation cartridges (catalog number 401959; Applied Biosystems). The filters were then treated with Biobrene, as recommended by the manufacturer. Sequencing was performed on an Applied Biosystems PROCISE™ 492 protein sequencer configured to utilize one-sixth of each cycle of Edman degradation for amino acid quantification and to collect the other five-sixths for ³H counting. To determine the amount of sequenced peptide, the pmol of each amino acid in a detected sequence was quantified by peak height and fit to the equation $f(x) = I_0R^x$, where I_0 represents the initial amount of the peptide sequenced (in pmol), R is the repetitive yield, and $f(x)$ is the pmol detected in cycle x . Ser, His, Trp, and Cys were not included in the fits due to known problems with their accurate detection/quantification. The fit was calculated in Sigma-

Binding Modes of [³H]Epibatidine to Muscle and Neuronal nAChRs

Plot 11 using a non-linear least squares method, and figures containing ³H release profiles include this fit as a *dotted line*. Some sequencing samples were treated with *o*-phthalaldehyde (OPA) prior to a cycle known to contain a proline (29). OPA

reacts with all amino-terminal amino acids (but not with the imino acid proline) and blocks further Edman degradation (30). Thus, release of ³H in a cycle after an OPA treatment establishes that the ³H release originates from a peptide with a proline in the OPA-treated cycle. Quantification of ³H incorporated into a specific residue (cpm/pmol) was calculated by $(\text{cpm}_x - \text{cpm}_{(\alpha-1)})/5I_0R^x$.

Molecular Modeling—Models of the extracellular domain of the human ($\alpha 4$)₂($\beta 2$)₃ and *Torpedo* nAChR were constructed from the x-ray structure of the epibatidine-bound form of the *Aplysia* AChBP (12) (Protein Data Bank code 2BYQ) using the Discovery Studio (Accelrys, Inc.) software package. Epibatidine (volume 156 Å³) was docked into the ABS of the *Aplysia* AChBP crystal structure and in the models of the *Torpedo* α - γ and human $\alpha 4$ - $\beta 2$ ABS using CDOCKER (31, 32), a CHARMM-based (33) molecular dynamics simulated annealing program that treats the ligand as fully flexible while maintaining a rigid receptor. In each docking experiment, 50 replicas of epibatidine (protonated form) were seeded in random orientations within the ABS defined by a binding site sphere of 12 Å radius. For each starting seed, CDOCKER was used to generate 10 ligand conformations using high temperature molecular dynamics, and then the 10 lowest energy orientations were identified using random rigid body rotations, followed by simulated annealing and a full potential final minimization step. For visualization, we show in Fig. 7 the Connolly surface representations, defined by a 1.8-Å diameter probe, of the ensemble of the 20 docking solutions with the lowest CDOCKER interaction energies.

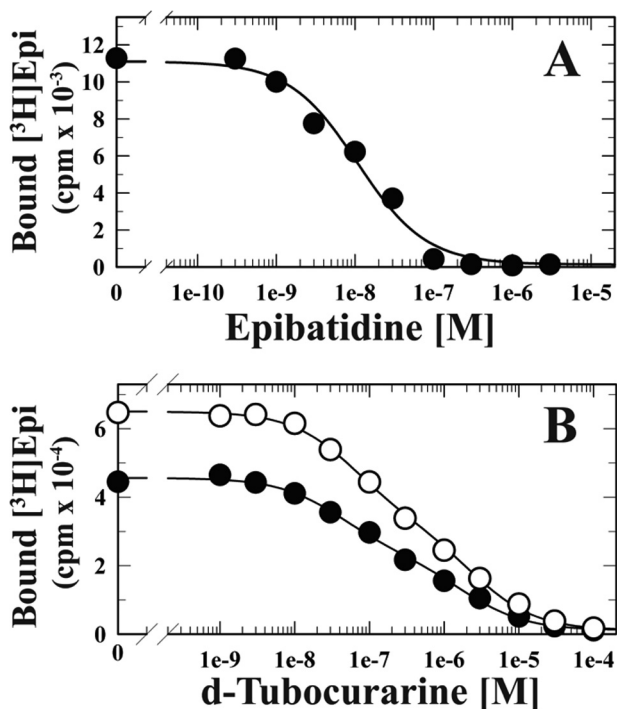


FIGURE 2. [³H]Epibatidine binds with high affinity at the two *Torpedo* nAChR ACh-binding sites. *A*, effect of epibatidine on the equilibrium binding of [³H]epibatidine (0.5 nM) to *Torpedo* nAChR-rich membranes (●). The inhibition of [³H]epibatidine binding was well fit by a single-site model with an IC₅₀ of 11 ± 2 nM. *B*, effect of dTC on the equilibrium binding of [³H]epibatidine (2 nM) to *Torpedo* nAChR-rich membranes in the absence (●) or presence (○) of 10 μM proadifen. The inhibition of [³H]epibatidine was well fit by a two-site model (–proadifen, IC₅₀ values 42 ± 7 nM and 1.8 ± 0.2 μM; +proadifen, IC₅₀ values 61 ± 7 nM and 2.4 ± 0.2 μM). Nonspecific binding was determined in the presence of 1 mM carbamylcholine.

RESULTS

[³H]Epibatidine Binding to *Torpedo* nAChR—In equilibrium binding studies with *Torpedo* nAChR-rich membranes, epibatidine fully inhibited the binding of 0.5 nM [³H]epibatidine, with the data well fit by a single-site model with an IC₅₀ of 11 ± 2 nM (Fig. 2*A*). We used the displacement of [³H]epibatidine binding by dTC to explore the agonist binding site selectivity of epibatidine.

dTC binds with higher affinity ($K_d = 35$ nM) at the *Torpedo* α - γ agonist binding site than the α - δ site ($K_d = 8$ μM) (34). The dTC displacement data (Fig. 2*B*, closed circles) were well fit by a model of two sites, equally occupied by [³H]epibatidine, with IC₅₀ values of 42 ± 7 nM and 1.8 ± 0.2 μM, consistent with dTC displacement of [³H]epibatidine bound to the α - γ and α - δ sites, respectively. The addition of proadifen, a desensitizing noncompetitive antagonist, enhanced [³H]epibatidine binding (Fig. 2*B*, open circles) with little effect on the relative occupancy by epibatidine of the α - γ and α - δ sites.

Photoincorporation of [³H]Epibatidine into *Torpedo* nAChR—We used SDS-PAGE followed by fluorography (Fig. 3*A*) and scintillation

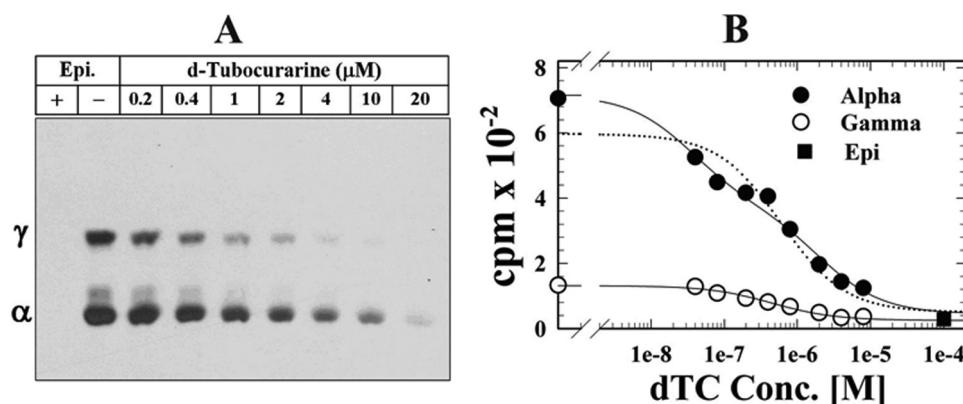


FIGURE 3. Photoincorporation of [³H]epibatidine into the *Torpedo* nAChR. Affinity-purified *Torpedo* nAChR (50 μg in 1 ml of VDB) was photolabeled with 0.13 μM [³H]epibatidine in the absence or presence of 40 μM epibatidine or increasing concentrations of dTC. *A*, fluorograph of an 8% SDS-polyacrylamide gel showing [³H]epibatidine photoincorporation into the α and γ subunits (–Epi lanes) that is inhibitable by epibatidine (+Epi lane) or dTC (0.2–20 μM lanes). *B*, ³H incorporation into the α and γ subunits, as determined by liquid scintillation counting of excised gel bands after fluorography. dTC inhibition of γ subunit labeling (○) was fit to a single-site model (IC₅₀ = 0.45 ± 0.07 μM), whereas inhibition of α subunit labeling (●) was better fit by a two-site model (solid line; IC₅₀ values 35 ± 12 nM and 2 ± 0.4 μM) than to a one-site model (dotted line; IC₅₀ = 0.6 ± 0.2 μM). Nonspecific labeling was determined in the presence of 40 μM epibatidine (■). In the absence of dTC, 710, 130, and 40 cpm were incorporated in the α , γ , and δ subunits, and 40, 25, and 25 were incorporated while in the presence of 40 μM epibatidine.

counting of excised gel bands (Fig. 3B) to provide an initial characterization of the subunit and pharmacological specificity of ³H incorporation when affinity-purified *Torpedo* nAChRs were photolabeled on an analytical scale (~50- μ g samples). As seen in the fluorograph, [³H]epibatidine was incorporated primarily in the nAChR α and γ subunits (*-Epi* lane). Photolabeling was eliminated by the addition of an excess (40 μ M) of nonradioactive epibatidine (*+Epi* lane) and inhibited in a concentration-dependent manner by dTC. Based upon scintillation counting, the concentration dependence of dTC inhibition of ³H photoincorporation in the γ subunit (Fig. 3B, *open circles*) was well fit by a single-site model with an IC₅₀ value of $0.45 \pm 0.07 \mu$ M, whereas inhibition of labeling in the α subunit (Fig. 3B, *solid circles*) was better fit by a two-site model (IC₅₀ values of 35 ± 12 nM and $2 \pm 0.4 \mu$ M) than a one-site model (IC₅₀ = $0.6 \pm 0.2 \mu$ M), where there were systematic deviations of the data from the fit at concentrations below 0.3 μ M. Pharmacologically specific (epibatidine-inhibitable) ³H photoincorporation within the δ subunit, if it occurred, was at <10% the level in the γ subunit. Although these labeling studies were conducted with affinity-purified nAChRs, an [³H]epibatidine photolabeling of native *Torpedo* nAChR-rich membranes under similar conditions also resulted in labeling of α and γ subunits, with little if any labeling in the δ subunit (data not shown).

Identification of Amino Acids Photolabeled by [³H]Epibatidine in the *Torpedo* α and γ Subunits—To identify amino acids photolabeled by [³H]epibatidine within the α and γ subunits, the incorporation in each subunit was first mapped by in-gel digestion with V8 protease, which for the α subunit produces fragments of ~20 kDa (α V8-20, beginning at α Ser¹⁷³ and containing ACh binding site Segment C), ~18 kDa (α V8-18, beginning at α Thr⁵² and containing binding site Segments A and B), and ~10 kDa (α V8-10, beginning at α Asn³³⁸ and containing the M4 membrane-spanning helix (35)). The corresponding fluorograph of a mapping gel (Fig. 4) established that all detectable (and specific) labeling in the α subunit was contained within a Coomassie-stained band of ~20 kDa (α V8-20), whereas, based upon liquid scintillation counting, the labeling in α V8-18 was less than 5% that of α V8-20 (supplemental Fig. S1). For the γ subunit, all ³H incorporation was contained within an ~14 kDa band (γ V8-14).

To identify the residues photolabeled by [³H]epibatidine, α V8-20 and γ V8-14 were isolated from affinity-purified *Torpedo* nAChRs photolabeled on a preparative scale (3.5 mg). Labeled α V8-20 was digested with EndoLys-C, which cleaves α V8-20 after α Lys¹⁸⁵ (36). When the digest was fractionated by rpHPLC, ~90% of the recovered ³H eluted in a single peak at ~87% solvent B (supplemental Fig. S1). Sequence analysis of the peak fractions (Fig. 5A) revealed a primary sequence beginning at α His¹⁸⁶ (23 pmol) and a single peak of ³H release in cycle 13, corresponding to labeling of α Tyr¹⁹⁸ (28 cpm/pmol), one of two tyrosines in Segment C contributing to the core aromatic binding pocket for ACh. During sequencing, the sample was treated after cycle 8 (see the *arrow* in Fig. 5A) with OPA, which reacts with primary, but not secondary, amines and blocks Edman degradation of any peptide without an amino-terminal proline at the time of addition (29, 30). The only sequence

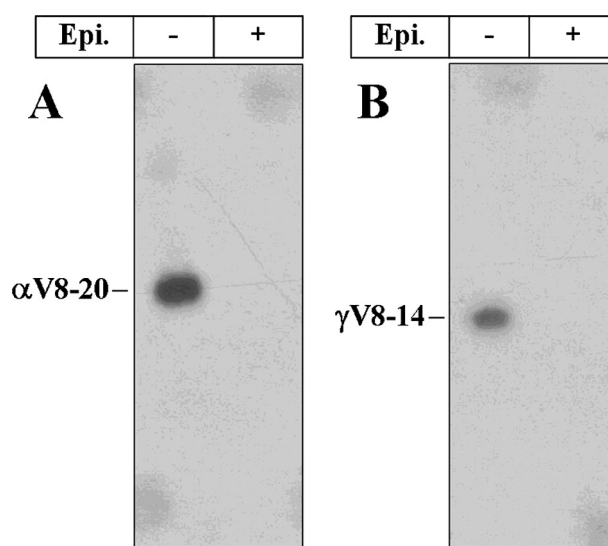


FIGURE 4. Mapping the sites(s) of [³H]epibatidine photoincorporation in the *Torpedo* nAChR α and γ subunits using V8 protease. Affinity-purified *Torpedo* nAChR (50 μ g) was photolabeled with 0.13 μ M [³H]epibatidine in the absence (*-Epi*) or presence (*+Epi*) of 40 μ M epibatidine. nAChR subunits were separated by SDS-PAGE (8% acrylamide gel), and the stained subunits were excised and subjected to in-gel digestion with V8 protease, as described under "Experimental Procedures." Fluorographs of α (A) and γ (B) subunit mapping gels (3-week exposure), showing [³H]epibatidine photoincorporation within polypeptides of ~20 kDa (α V8-20) and 14 kDa (γ V8-14), respectively (*-lanes*) that is inhibitable by epibatidine (*+lanes*).

detected after cycle 8 was the primary sequence (with α Pro¹⁹⁴ in cycle 9), providing additional evidence that the ³H release in cycle 13 resulted from [³H]epibatidine incorporation into α Tyr¹⁹⁸.

When [³H]epibatidine-labeled γ V8-14 was further purified by rpHPLC, ~80% of the recovered ³H eluted in a single peak at ~57% solvent B (supplemental Fig. S1). Sequence analysis of the pooled peak fractions (Fig. 5B) revealed a single sequence beginning at γ Val¹⁰² (55 pmol) with ³H release in cycles 8 and 16, corresponding to labeling of γ Leu¹⁰⁹ (23 cpm/pmol) and γ Tyr¹¹⁷ (13 cpm/pmol), residues located within Segment E of the agonist binding site previously identified by photoaffinity labeling (20).

Photoincorporation of [³H]Epibatidine into α 4 β 2 nAChR—Affinity-purified neuronal α 4 β 2 nAChRs were photolabeled on an analytical scale (~50- μ g samples) with 880 nM [³H]epibatidine in the absence and presence of excess nonradioactive epibatidine (40 μ M), and the ³H incorporation was assessed by SDS-PAGE and fluorography (Fig. 6). [³H]epibatidine photoincorporated primarily into the α 4 subunit and in a broad band migrating with an apparent molecular mass of ~36 kDa, with low level labeling of the β 2 subunit, and labeling in each band was fully inhibited by epibatidine. Based upon liquid scintillation counting of excised gel bands, 1,600, 550, and 2,400 cpm were incorporated into the α 4 and β 2 subunits and 36 kDa band, respectively, and photolabeling in each band was inhibited by >95% by excess nonradioactive epibatidine. Based on previous studies with purified α 4 β 2 nAChRs (26), the [³H]epibatidine-labeled material migrating at ~36 kDa probably included proteolytic fragments of both the α 4 and β 2 subunits, which was confirmed by protein sequencing (supplemental Fig. S2).

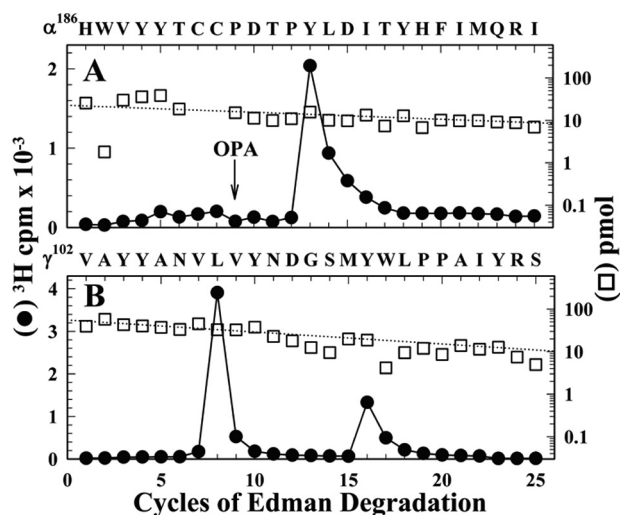


FIGURE 5. Identification of *Torpedo* nAChR amino acids photolabeled by [³H]epibatidine. Affinity-purified *Torpedo* nAChR (3.5 mg in 8 ml) was photolabeled with 550 nm [³H]epibatidine, nAChR subunits were separated by SDS-PAGE (8% acrylamide gel), and the stained α and γ subunits bands were excised and digested in gel with V8 protease on a second gel, as described under "Experimental Procedures." Material eluted from α V8-20 was digested with EndoLys-C and then fractionated by HPLC, whereas material eluted from γ V8-14 was purified directly by HPLC (supplemental Fig. S1). A, ³H (●) and PTH-derivatives (□) released during amino acid sequence analysis of the ³H peak (fractions 34–36; 31,000 cpm) from the HPLC purification of the EndoLys-C digest of α V8-20. During sequencing, the filter was treated with OPA before cycle 9 (indicated by an arrow) to chemically isolate the primary peptide detected (α His¹⁸⁶, $l_0 = 23 \pm 9$ pmol, $r = 96\%$, with α Pro¹⁹⁴ in cycle 9) by preventing further sequencing of fragments not containing a proline in this cycle (29, 30). The only sequence detected after cycle 8 was the primary sequence, establishing that the ³H release in cycle 15 resulted from [³H]epibatidine incorporation into α Tyr¹⁹⁸ (28 cpm/pmol). B, ³H (●) and PTH-derivatives (□) released during amino acid sequence analysis of the ³H peak (fractions 28–30; 22,500 cpm) from the HPLC purification of γ V8-14. The only fragment detected began at γ Val¹⁰² ($l_0 = 55 \pm 5$ pmol, $r = 94\%$) and was present at >20-fold higher amount than any other sequences. The ³H releases in cycles 8 and 16 correspond to photolabeling of γ Leu¹⁰⁹ (23 cpm/pmol) and γ Tyr¹¹⁷ (13 cpm/pmol).

Identification of Amino Acids Photolabeled by [³H]Epibatidine in the α 4 β 2 nAChR—To identify specific residues labeled by [³H]epibatidine in the α 4 and β 2 subunits, each subunit was isolated from α 4 β 2 nAChRs labeled on a preparative scale (1.2 mg of nAChR; 800 nM [³H]epibatidine). Labeled subunits were digested with V8 protease for 4 days, and the digests were fractionated by rpHPLC. When the α 4 subunit digest was fractionated by rpHPLC (Fig. 7A), the ³H eluted in peaks centered at fraction 25 (~50% solvent B) and fraction 28 (~57% solvent B) and in the column flow-through.⁴ Sequence analysis of the pool of fractions 24–26 (Fig. 7B) revealed a fragment beginning at α 4Trp¹⁸¹ (5 pmol) as well as the amino terminus of V8 protease, which was the primary sequence. The major peak of ³H release in cycle 15 corresponded to labeling of α 4Tyr¹⁹⁵ (10 cpm/pmol), a residue that is contained within Segment C of the ABS and is equivalent to α Tyr¹⁹⁰ of the muscle-type nAChR.

When the V8 digest of the photolabeled nAChR β 2 subunit was fractionated by rpHPLC (Fig. 7C), ³H cpm eluted in a peak

⁴ The ³H cpm released in the column flow-through (fractions 1–4) during the HPLC purification of the V8 digest of α 4 and β 2 subunits was later determined to result from a defect in the Brownlee Aquapore C₄ column rather than the presence of [³H]epibatidine-labeled peptides that elute at a very low percentage of solvent B.

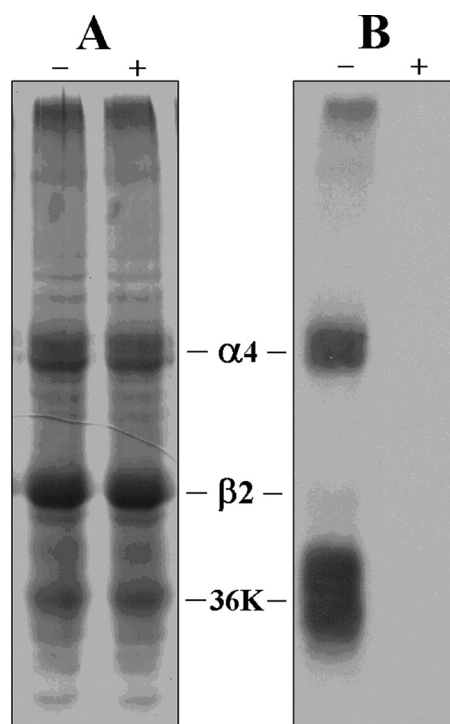


FIGURE 6. Photoincorporation of [³H]epibatidine into the α 4 β 2 nAChR. Affinity-purified α 4 β 2 nAChR (~50 μ g of protein) reincorporated into lipid was photolabeled with 880 nm [³H]epibatidine in the absence (–Epi lane) or presence of 40 μ M epibatidine (+Epi lane). Polypeptides were then resolved by SDS-PAGE, visualized by Coomassie Blue stain (A), and processed for fluorography (B) (3-week exposure). The electrophoretic mobilities of the α 4 and β 2 subunits and the ³H-labeled proteolytic fragments of ~36 kDa are indicated.

centered at fraction 28 (~55% solvent B) and in column flow-through. Sequence analysis of the pool of fractions 27–29 (Fig. 7D) revealed a β 2 subunit fragment beginning at β 2Val¹⁰⁴ (19 pmol) in addition to the V8 protease amino terminus, which was the primary sequence. The peaks of ³H release in cycles 8 and 10 indicate [³H]epibatidine photolabeling of β 2Val¹¹¹ (2 cpm/pmol) and β 2Ser¹¹³ (~0.3 cpm/pmol), residues that are contained within Segment E of the agonist binding domain. Sequence analysis of the V8 protease digest of the [³H]epibatidine-labeled 36 kDa band (supplemental Fig. S2) revealed the presence of nAChR subunit fragments beginning at α 4Trp¹⁸¹ and at β 2Val¹⁰⁴, with ³H cpm release in cycles 8, 10, and 15, consistent with labeling of β 2Val¹¹¹, β 2Ser¹¹³, and α 4Tyr¹⁹⁵, respectively.

DISCUSSION

In this report, we use the intrinsic photoreactivity of the nAChR agonist [³H]epibatidine to compare its mode of binding in the *Torpedo* and neuronal α 4 β 2 nAChRs. Although the reactive intermediates formed upon photolysis of epibatidine have not been directly identified, halo pyridines, such as the chlorinated pyridine ring of epibatidine, are known to undergo photoaddition reactions initiated by the cleavage of the C–Cl bond (37–39), and it is that carbon that is probably reactive in epibatidine. Irradiation at 254 nm results in [³H]epibatidine photoincorporation into the α 4- β 2 and *Torpedo* α - γ ABS, with little or no labeling detected in regions outside of that domain. Likely contributors to the high specificity of [³H]epibatidine labeling

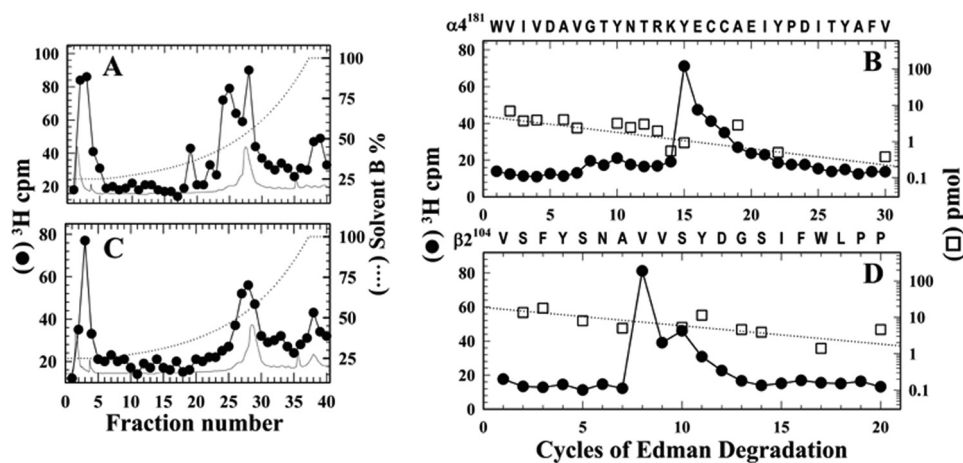


FIGURE 7. Identification of $\alpha 4\beta 2$ nAChR amino acids photolabeled by [³H]epibatidine. Reversed-phase HPLC fractionation (A and C) and amino acid sequence analysis (B and D) of in-solution V8 protease digests of the $\alpha 4$ (A and B) and $\beta 2$ (C and D) subunits isolated from [³H]epibatidine-labeled affinity-purified $\alpha 4\beta 2$ nAChR (1.2 mg $\alpha 4\beta 2$ nAChR, 800 nM [³H]epibatidine). The elution of peptides during HPLC was monitored by absorbance at 210 nm (solid line), and ³H elution was quantified by liquid scintillation counting of 5% of each fraction (●). B, ³H (●) and PTH-derivatives (○) released during amino acid sequence analysis of ³H peak (fractions 24–26; 4,200 cpm) from the HPLC purification of the V8 protease digest of the $\alpha 4$ subunit. The primary peptides detected began at $\alpha 4\text{Trp}^{181}$ ($I_0 = 5 \pm 0.3$ pmol, $r = 90\%$) and at the amino terminus of V8 protease (~10 pmol), with a peak of ³H release in cycle 15 corresponding to labeling of $\alpha 4\text{Tyr}^{195}$ (10 cpm/pmol). For the material in HPLC fraction 28, which coeluted with a major peak of UV absorbance, the amino terminus of V8 protease was the dominant sequence, and no ³H release was detected in 30 cycles of Edman degradation (not shown). D, ³H (●) and PTH-derivatives (□) released during amino acid sequence analysis of the ³H peak (fractions 27–29; 3,100 cpm) from the HPLC purification of the V8 protease digest of the $\beta 2$ subunit. The primary peptides detected began at $\beta 2\text{Val}^{104}$ ($I_0 = 19 \pm 3$ pmol, $r = 89\%$) and at the amino terminus of V8 protease, with ³H release in cycles 8 and 10 corresponding to labeling of $\beta 2\text{Val}^{111}$ (1.9 cpm/pmol) and $\beta 2\text{Ser}^{113}$ (~0.3 cpm/pmol).

include the very high binding affinity to $\alpha 4\beta 2$ nAChRs (~100 pM) (40) and the molecular rigidity of epibatidine. In contrast to photolabeling studies conducted with the iodo-analog of epibatidine ([¹²⁵I]epibatidine) (41), the amino acids in the ABS of the $\alpha 4\beta 2$ and *Torpedo* nAChRs that reacted with [³H]epibatidine were readily identified by Edman degradation.

In the *Torpedo* nAChR, our results establish that [³H]epibatidine binds to both the α - γ and α - δ ABS with high affinity (~11 nM). Although epibatidine may bind with 3–4-fold higher affinity to one of the two sites in the *Torpedo* nAChR, as does ACh (42), it did not have the high selectivity between the sites seen in the mouse muscle nAChR (>170-fold higher affinity for the α - γ than the α - δ site in the desensitized state (43)). Despite its high affinity binding to the α - γ and α - δ ABS in the *Torpedo* nAChR, [³H]epibatidine photoincorporated into the α and γ subunits with little, if any, in the δ subunit. The concentration dependence of dTC inhibition of [³H]epibatidine photolabeling of the α subunit indicated that both α subunits may be photolabeled, but further studies at higher [³H]epibatidine concentrations would be necessary to identify possible photolabeling in the δ subunit. Within the α and γ subunits, photolabeling was restricted to amino acids within binding site Segments C (α) and E (γ), with αTyr^{198} (28 cpm/pmol), γLeu^{109} (23 cpm/pmol), and γTyr^{117} (13 cpm/pmol) labeled most efficiently. [³H]Epibatidine photolabeling at the subunit level and within the α subunit mirrors that observed with [³H]nicotine photoincorporation into the *Torpedo* nAChR (29) but not within the γ subunit. [³H]Epibatidine did not photolabel γTrp^{55} , the primary amino acid labeled by [³H]nicotine (44).

In the $\alpha 4\beta 2$ nAChR, [³H]epibatidine photolabeled the $\alpha 4$ subunit at ~3-fold higher efficiency than the $\beta 2$ subunit, and

consistent with this, [³H]epibatidine photolabeled $\alpha 4\text{Tyr}^{195}$ (10 cpm/pmol; equivalent to *Torpedo* αTyr^{190}) in Segment C more efficiently than the two labeled amino acids in the $\beta 2$ subunit: $\beta 2\text{Val}^{111}$ (2 cpm/pmol) and $\beta 2\text{Ser}^{113}$ (~0.6 cpm/pmol) in Segment E (equivalent to *Torpedo* γLeu^{109} and γTyr^{111} , respectively). Tomizawa *et al.* (21) reported that [³H]azidoepibatidine also photolabeled the $\alpha 4$ subunit more efficiently (no labeling of the $\beta 2$ subunit was evident by fluorography), although the photolabeled amino acids were not identified. Although [³H]epibatidine photolabeled αTyr^{198} in the *Torpedo* nAChR and azidoepibatidine photolabeled the corresponding position (Tyr¹⁹⁵) in the *Aplysia* AChBP (21), that position was not labeled in the $\alpha 4$ subunit, whereas the position corresponding to αTyr^{190} was labeled. Within the γ and $\beta 2$ subunits, [³H]epibatidine labeled equivalent positions

($\gamma\text{Leu}^{109}/\beta 2\text{Val}^{111}$) most efficiently. The position equivalent to the *Aplysia* AChBP Met¹¹⁶, which was labeled by azidoepibatidine, was labeled in the *Torpedo* nAChR (γTyr^{117}) at 50% of the efficiency of γLeu^{109} , but any labeling of the corresponding position in the $\alpha 4\beta 2$ nAChR ($\beta 2\text{Phe}^{119}$), if it occurred, was at <10% the efficiency of $\beta 2\text{Val}^{111}$.

Proposed Orientations of Epibatidine in the Torpedo and alpha4beta2 nAChR Agonist Binding Sites from Photolabeling and Molecular Modeling—As one approach to identify factors that could explain the selective labeling of non-equivalent core aromatic amino acids within Segment C of the *Torpedo* (αTyr^{198}) and $\alpha 4\beta 2$ ($\alpha 4\text{Tyr}^{195}$) ABS by what must be the same epibatidine photoreactive intermediate, we used computational methods to predict favored epibatidine docking orientations in the ABS in homology models of the *Torpedo* and $\alpha 4\beta 2$ nAChRs based on the structure of the epibatidine-bound form of *Aplysia* AChBP (12). When epibatidine was docked in the *Torpedo* α - γ ABS, a single binding orientation was highly favored (Fig. 8A) that was essentially the same as epibatidine in the crystal structure of the ligand-bound form of AChBP (12) and as we found for epibatidine docked in the AChBP crystal structure (not shown) or had been found for epibatidine docked in a structural model of chick $\alpha 7$ nAChR (45). In this orientation, the azabicycloheptane ring occupies the “aromatic box” formed by αTyr^{93} , αTyr^{190} , αTyr^{198} , αTyr^{149} , and γTrp^{55} , and the chloropyridyl ring is oriented toward Segment E, with C6 of the pyridyl ring (the most likely reactive site) positioned within 6 Å of the labeled αTyr^{198} , γTyr^{117} , and γLeu^{109} but 11 Å from the unlabeled αTyr^{190} (Fig. 8B).

When epibatidine was docked into the ABS of the $\alpha 4\beta 2$ nAChR homology model, two distinct binding orientations

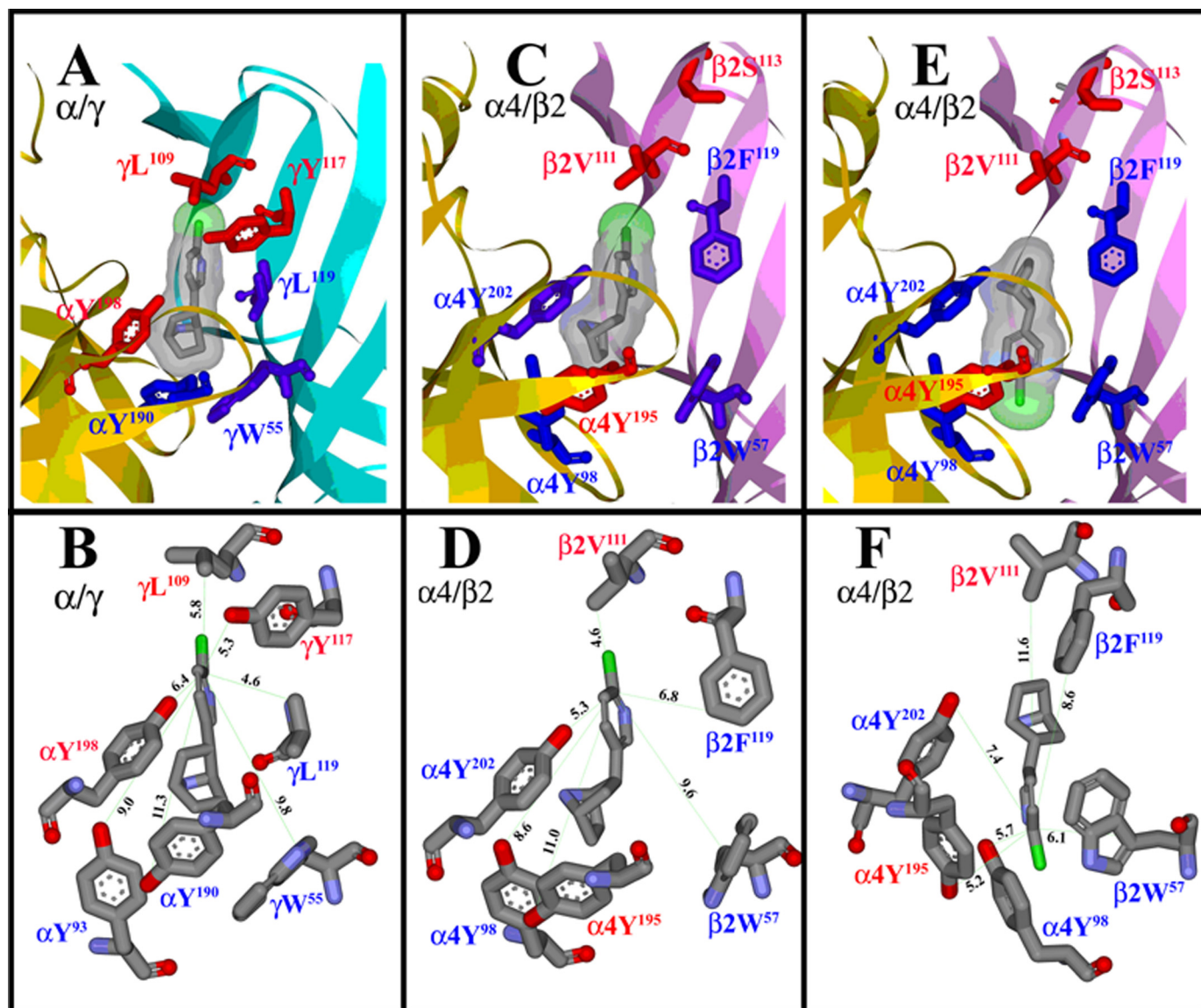


FIGURE 8. Molecular models of epibatidine docked in the *Torpedo* α - γ and α 4 β 2 nAChR agonist binding sites. Epibatidine was docked into the ABS of the *Torpedo* α - γ (A and B) and human α 4- β 2 (C-F) homology models using CDOCKER, as described under "Experimental Procedures." A, C, and E, views of the α - γ (A) and α 4- β 2 (C and E) ABS in a flat ribbon representation (gold, α and α 4; cyan, γ ; pink, β 2) showing Connolly surface of the ensemble of the 20 lowest energy solutions of epibatidine, which docked in a single orientation in the α - γ ABS and in two orientations in the α 4- β 2 ABS, one orientation (C) similar to that in the α - γ ABS, and a second orientation rotated by $\sim 180^\circ$ and translated by 3 Å. In each image, the lowest energy epibatidine orientation and amino acids within the ABS are shown in stick format with the [³H]epibatidine-labeled amino acids colored red and unlabeled amino acids in blue. B, D, and F, the distances in Å between the C6 of the chloropyridyl ring of epibatidine and amino acids within the ABS for A, C, and E, respectively. The colors reflect atom type: carbon (black), oxygen (red), nitrogen (blue), and chlorine (green). See supplemental Fig. S3 for an alternative view of α 4 β 2 ABS that highlights the orientations of epibatidine relative to α 4Trp¹⁴³.

were predicted with similar energy and frequency: one orientation similar to that seen in the *Torpedo* α - γ ABS (Fig. 8C; *up orientation* with reference to the position of chlorine) and a second orientation with epibatidine rotated by $\sim 180^\circ$ and translated by 3 Å, orienting the chloropyridyl ring toward the core aromatic side chains (Fig. 8E; *down orientation*). In both orientations, the positively charged nitrogen in the azabicycloheptane ring is located 2.6 Å from the backbone carbonyl group of α 4Trp¹⁴³ and ~ 4.6 Å from the aromatic side chain (supplemental Fig. S3), preserving equivalent potential for the hydrogen bonding and/or cation- π interactions predicted to be important determinants of binding affinity (9, 12, 14, 15). In both orientations, the positively charged nitrogen is also ~ 4 Å

from α 4Tyr²⁰², which was not photolabeled by [³H]epibatidine. In the *up orientation* (Fig. 8C), the pyridyl C6 is positioned ~ 5 Å from the labeled β 2Val¹¹¹ but 11 Å from the labeled α 4Tyr¹⁹⁵ (Fig. 8D). In the *down orientation* (Fig. 8E), the pyridyl C6 is positioned ~ 5 Å from the labeled α 4Tyr¹⁹⁵ but 12 Å from the labeled β 2Val¹¹¹ (Fig. 8F). These simple proximity relations suggest that epibatidine is likely to bind in an *up orientation* when β Val¹¹¹ is labeled and in a *down orientation* when α 4Tyr¹⁹⁵ is photolabeled.

Although only a single binding orientation has been seen for epibatidine and other agonists and antagonists in the *Aplysia* AChBP crystal structures (11, 12), mutational analyses have provided evidence that the competitive antagonist dTC and its

quaternary ammonium analog, metocurine, bind in distinctly different orientations in both the AChBP and the muscle nAChR (16, 17). Moreover, the prediction of two distinct epibatidine binding orientations in the $\alpha 4\beta 2$ ABS parallels the prediction that dTC and metocurine can bind in distinct orientations in the AChBP and human α - ϵ ABS, respectively (16, 17). Our interpretation is based upon a plausible, but unproven, assumption that cleavage of the C–Cl bond of epibatidine produces the only reactive intermediate, and it is also possible that the differences in the patterns of [³H]epibatidine photolabeling between the *Torpedo* and $\alpha 4\beta 2$ nAChRs result from differences in the structures of the transmitter binding sites between the two nAChRs, including the position and orientations of the core aromatic amino acids. However, the proposal that nAChR ligands bind in a “normal” and an “inverted” orientation provides a plausible explanation for our photolabeling results, as for photolabeling studies of neonicotinoids binding to the *Lymnaea* AChBP (46).

Acknowledgments—We thank Dr. David C. Chiara (Department of Neurobiology, Harvard Medical School) for advice and comments during the course of this study. We also thank Sarah Hiyari (Texas Tech University/Howard Hughes Medical Institute undergraduate fellow) for technical assistance.

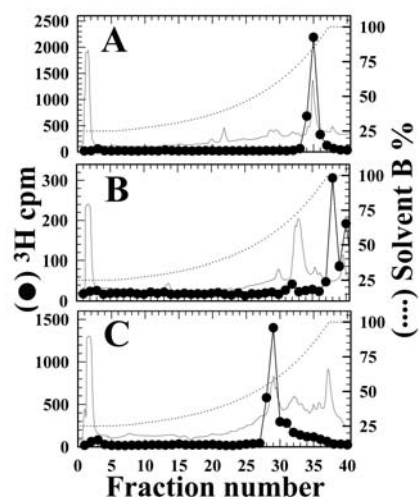
REFERENCES

- Albuquerque, E. X., Pereira, E. F., Alkondon, M., and Rogers, S. W. (2009) *Physiol. Rev.* **89**, 73–120
- Wells, G. B. (2008) *Front. Biosci.* **13**, 5479–5510
- Jensen, A. A., Frølund, B., Liljefors, T., and Krosgaard-Larsen, P. (2005) *J. Med. Chem.* **48**, 4705–4745
- Dani, J. A., and Bertrand, D. (2007) *Annu. Rev. Pharmacol. Toxicol.* **47**, 699–729
- Nelson, M. E., Kuryatov, A., Choi, C. H., Zhou, Y., and Lindstrom, J. (2003) *Mol. Pharmacol.* **63**, 332–341
- Moroni, M., Zwart, R., Sher, E., Cassels, B. K., and Bermudez, I. (2006) *Mol. Pharmacol.* **70**, 755–768
- Corringer, P. J., Le Novère, N., and Changeux, J. P. (2000) *Annu. Rev. Pharmacol. Toxicol.* **40**, 431–458
- Changeux, J.-P., and Edelman, S. J. (2005) *Nicotinic Acetylcholine Receptors: From Molecular Biology to Cognition*, Odile Jacob Publishing, New York, NY
- Dougherty, D. A. (2008) *Chem. Rev.* **108**, 1642–1653
- Brejč, K., van Dijk, W. J., Klaassen, R. V., Schuurmans, M., van Der Oost, J., Smit, A. B., and Sixma, T. K. (2001) *Nature* **411**, 269–276
- Celie, P. H., van Rossum-Fikkert, S. E., van Dijk, W. J., Brejč, K., Smit, A. B., and Sixma, T. K. (2004) *Neuron* **41**, 907–914
- Hansen, S. B., Sulzenbacher, G., Huxford, T., Marchot, P., Taylor, P., and Bourne, Y. (2005) *EMBO J.* **24**, 3635–3646
- Unwin, N. (2005) *J. Mol. Biol.* **346**, 967–989
- Cashin, A. L., Torrice, M. M., McMenimen, K. A., Lester, H. A., and Dougherty, D. A. (2007) *Biochemistry* **46**, 630–639
- Xiu, X., Nuskar, N. L., Shanata, J. A., Lester, H. A., and Dougherty, D. A. (2009) *Nature* **458**, 534–537
- Gao, F., Bern, N., Little, A., Wang, H. L., Hansen, S. B., Talley, T. T., Taylor, P., and Sine, S. M. (2003) *J. Biol. Chem.* **278**, 23020–23026
- Wang, H. L., Gao, F., Bren, N., and Sine, S. M. (2003) *J. Biol. Chem.* **278**, 32284–32291
- Kotzyba-Hibert, Kapfer, I., and Goeldner, M. (1995) *Angew. Chem. Int. Ed. Engl.* **34**, 1296–1312
- Vodovozova, E. L. (2007) *Biochemistry* **72**, 1–20
- Nirthanan, S., Ziebell, M. R., Chiara, D. C., Hong, F., and Cohen, J. B. (2005) *Biochemistry* **44**, 13447–13456
- Tomizawa, M., Maltby, D., Medzihradzky, K. F., Zhang, N., Durkin, K. A., Presley, J., Talley, T. T., Taylor, P., Burlingame, A. L., and Casida, J. E. (2007) *Biochemistry* **46**, 8798–8806
- Pedersen, S. E., Dreyer, E. B., and Cohen, J. B. (1986) *J. Biol. Chem.* **261**, 13735–13743
- Fong, T. M., and McNamee, M. G. (1986) *Biochemistry* **25**, 830–840
- Hamouda, A. K., Sanghvi, M., Sauls, D., Machu, T. K., and Blanton, M. P. (2006) *Biochemistry* **45**, 4327–4337
- Zhang, J., and Steinbach, J. H. (2003) *Brain Res.* **959**, 98–102
- Hamouda, A. K., Sanghvi, M., Chiara, D. C., Cohen, J. B., and Blanton, M. P. (2007) *Biochemistry* **46**, 13837–13846
- Laemmli, U. K. (1970) *Nature* **227**, 680–685
- Cleveland, D. W., Fischer, S. G., Kirschner, M. W., and Laemmli, U. K. (1977) *J. Biol. Chem.* **252**, 1102–1106
- Middleton, R. E., and Cohen, J. B. (1991) *Biochemistry* **30**, 6987–6997
- Brauer, A. W., Oman, C. L., and Margolies, M. N. (1984) *Anal. Biochem.* **137**, 134–142
- Wu, G., Robertson, D. H., Brooks, C. L., 3rd, and Vieth, M. (2003) *J. Comput. Chem.* **24**, 1549–1562
- Erickson, J. A., Jalaie, M., Robertson, D. H., Lewis, R. A., and Vieth, M. (2004) *J. Med. Chem.* **47**, 45–55
- Brooks, B. R., Bruccoleri, R. E., Olafson, B. D., States, D. J., Swaminathan, S., and Karplus, M. (1983) *J. Comput. Chem.* **4**, 187–217
- Neubig, R. R., and Cohen, J. B. (1979) *Biochemistry* **18**, 5464–5475
- White, B. H., and Cohen, J. B. (1988) *Biochemistry* **27**, 8741–8751
- Chiara, D. C., and Cohen, J. B. (1997) *J. Biol. Chem.* **272**, 32940–32950
- Whitten, D. G. (1976) in *Photochemistry of Heterocyclic Compounds* (Buchardt, O., ed) pp. 524–573, John Wiley & Sons, Inc., New York
- Ohkura, K., Seki, K., Terashima, M., and Kanaoka, Y. (1989) *Tetrahedron Lett.* **30**, 3433–3436
- Zoltewicz, J. A., and Locko, G. A. (1983) *J. Org. Chem.* **48**, 4214–4219
- Xiao, Y., and Kellar, K. J. (2004) *J. Pharmacol. Exp. Ther.* **310**, 98–107
- Hamouda, A. K., Sanghvi, M., Chiara, D. C., Srivastava, S., Cohen, J. B., and Blanton, M. P. (2008) *Biophys. J.* **94**, 1418a
- Song, X. Z., Andreeva, I. E., and Pedersen, S. E. (2003) *Biochemistry* **42**, 4197–4207
- Prince, R. J., and Sine, S. M. (1998) *J. Biol. Chem.* **273**, 7843–7849
- Chiara, D. C., Middleton, R. E., and Cohen, J. B. (1998) *FEBS Lett.* **423**, 223–226
- Le Novère, N., Grutter, T., and Changeux, J. P. (2002) *Proc. Natl. Acad. Sci. U.S.A.* **99**, 3210–3215
- Tomizawa, M., Maltby, D., Talley, T. T., Durkin, K. A., Medzihradzky, K. F., Burlingame, A. L., Taylor, P., and Casida, J. E. (2008) *Proc. Natl. Acad. Sci. U.S.A.* **105**, 1728–1732

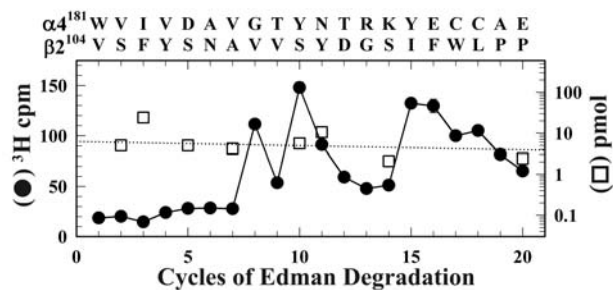
**[³H]EPIBATIDINE PHOTOLABELS NON-EQUIVALENT AMINO ACIDS IN
THE AGONIST BINDING SITE OF TORPEDO AND α 4 β 2 NICOTINIC
ACETYLCHOLINE RECEPTORS**

Shouryadeep Srivastava^{1*}, Ayman K. Hamouda^{2*}, Akash Pandhare¹, Phaneendra K. Duddempudi¹, Mitesh Sanghvi¹, Jonathan B. Cohen² and Michael P. Blanton¹

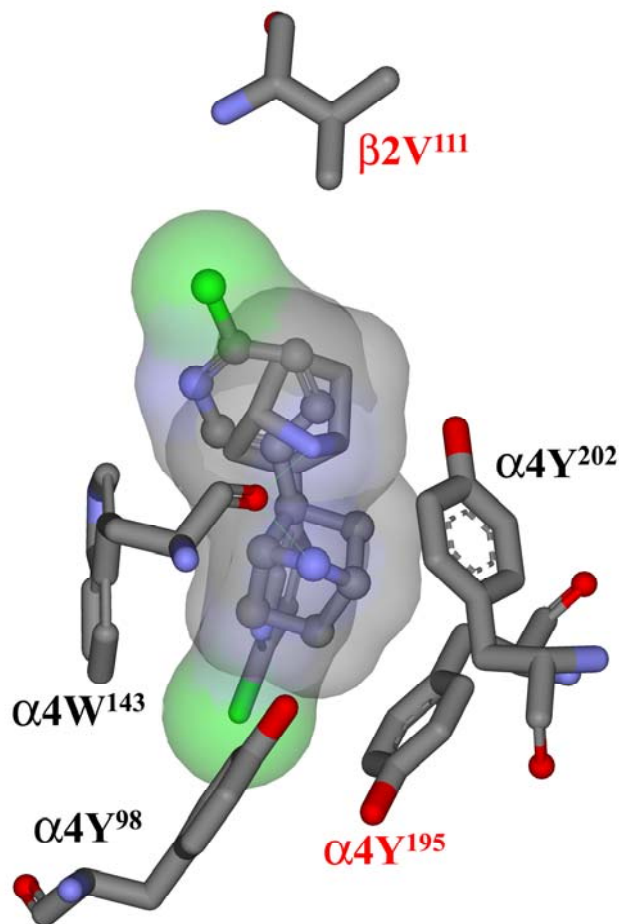
Supplementary Figures S1-S3



Supplementary Figure S1. Reversed-phase HPLC purification of [³H]Epibatidine labeled *Torpedo* V8 fragments α V8-20 (Endo-Lys-C digested), α V8-18, γ V8-14. From a preparative scale [³H]epibatidine labeling of the *Torpedo* nAChR, the V8 proteolytic fragments α V8-20 (A), α V8-18 (B), and γ V8-14 (C) were isolated, the α V8-20 fragment digested with Endo-Lys-C, and each fragment was then further purified by reversed-phase HPLC. A nonlinear elution gradient (dotted line) of solvent B (0.05% TFA in 60% acetonitrile/40% isopropanol) in solvent A (0.08% TFA in water) at a flow rate of 0.2 mL/min was employed. The elution of peptides was monitored by the absorbance at 210 nm (solid line). Fractions were collected every 2.5 min and ³H cpm associated with each fraction (●) was determined by liquid scintillation counting. For the rpHPLC elution profile of α V8-18 (B), the α V8-18 peptide (starting at α Thr⁵² and containing binding site segments A and B) is found within fractions 31-33 and contains ~2,000 cpm. This indicates that the extent of [³H]epibatidine labeling in α V8-18 is less than 5% of that found within α V8-20 (A, fractions 34-36, 64,000 cpm). In addition, the ³H cpm found in fractions 38-40 for the rpHPLC separation of α V8-18 (B), was shown to contain undigested α V8-20 peptide, indicating that this material co-migrated with the α V8-18 band on the 15% mapping gel.



Supplementary Figure S2. Identification of $\alpha 4\beta 2$ nAChR amino acids photolabeled by $[^3\text{H}]$ Epibatidine in the 36 kDa band. ^3H (●) and mass release (□) detected during sequence analysis of the peak of ^3H (fractions 25-28 from the HPLC purification of the V8 protease digest of materials isolated from the 36 kDa gel band of the $\alpha 4\beta 2$ preparative photolabeling of Figure 7 (10,440 cpm loaded on the filter, 1,000 cpm remaining after 20 cycles). Aside from that of V8 protease, both $\alpha 4$ and $\beta 2$ peptides were detected ($\alpha 4\text{Trp}^{181}$, $I_0 = 6$ pmol; $\beta 2\text{Val}^{104}$, $I_0 = 4$ pmol) and ^3H cpm release was evident in cycles 8, 10, and 15 consistent with labeling of $\beta 2\text{Val}^{111}$, $\beta 2\text{Ser}^{113}$, and $\alpha 4\text{Tyr}^{195}$ respectively.



Supplementary Figure S3. Epibatidine docks in the $\alpha 4\beta 2$ agonist binding site in two orientations. A view of the two orientations of epibatidine docked in the $\alpha 4$ – $\beta 2$ agonist binding site: the “up” orientation shown in ball and stick format and the “down” orientation shown in stick format (from Figures 8C and E). Shown also, for each orientation, is a Connolly surface of the ensemble of the 20 docking solutions with the most favorable CDOCKER interaction energies, as well as amino acids $\alpha 4\text{Tyr}^{202}$, $\alpha 4\text{Tyr}^{195}$, $\alpha 4\text{Tyr}^{98}$, $\alpha 4\text{Trp}^{143}$, and $\beta 2\text{Val}^{111}$ in stick format. In both orientations the positively charged nitrogen in the azabicycloheptane ring is located 2.6 Å from the backbone carbonyl group and ~4.6 Å from the aromatic side of $\alpha 4\text{Trp}^{143}$. Colors reflect atom type: carbon, black; oxygen, red; nitrogen, blue; chlorine, green.